Cell Reports
Article

Organization of Monosynaptic Inputs to the Serotonin and Dopamine Neuromodulatory Systems

Sachie K. Ogawa,[1] Jeremiah Y. Cohen,[1,2,*] Dabin Hwang,[1] Naoshige Uchida,[1] and Mitsuko Watabe-Uchida[1,*]
[1]Center for Brain Science, Department of Molecular and Cellular Biology, Harvard University, 16 Divinity Avenue, Cambridge, MA 02138, USA
[2]Present address: The Solomon H. Snyder Department of Neuroscience, Brain Science Institute, The Johns Hopkins University School of Medicine, Baltimore, MD 21205, USA
*Correspondence: jeremiah.cohen@jhmi.edu (J.Y.C.), mitsuko@mcb.harvard.edu (M.W.-U.)
http://dx.doi.org/10.1016/j.celrep.2014.06.042

SUMMARY

Serotonin and dopamine are major neuromodulators. Here, we used a modified rabies virus to identify monosynaptic inputs to serotonin neurons in the dorsal and median raphe (DR and MR). We found that inputs to DR and MR serotonin neurons are spatially shifted in the forebrain, and MR serotonin neurons receive inputs from more medial structures. Then, we compared these data with inputs to dopamine neurons in the ventral tegmental area (VTA) and substantia nigra pars compacta (SNc). We found that DR serotonin neurons receive inputs from a remarkably similar set of areas as VTA dopamine neurons apart from the striatum, which preferentially targets dopamine neurons. Our results suggest three major input streams: a medial stream regulates MR serotonin neurons, an intermediate stream regulates DR serotonin and VTA dopamine neurons, and a lateral stream regulates SNc dopamine neurons. These results provide fundamental organizational principles of afferent control for serotonin and dopamine.

INTRODUCTION

Serotonin and dopamine are major neuromodulators essential for flexible behavior. Both are released from small populations of neurons in the midbrain and brainstem. A unique feature of these neurons is that they receive and integrate inputs from many brain areas, and broadcast their outputs through long axons to many brain areas (Jacobs and Azmitia, 1992). Despite the importance of these neurotransmitters in normal behaviors and psychiatric disorders, their regulation remains poorly understood.

Forebrain-projecting serotonin neurons are found in the dorsal raphe (DR) and median raphe (MR). They are thought to be involved in diverse functions including the regulation of sleep-wake cycles (Lydic et al., 1983; McGinty and Harper, 1976), motor facilitation (Jacobs and Fornal, 1997), defensive behavior (Deakin and Graeff, 1991), behavioral inhibition (Soubrie, 1986), learning from negative reinforcement (Daw et al., 2002; Dayan and Huys, 2008; Deakin and Graeff, 1991; den Ouden et al., 2013), processing reward value (Nakamura et al., 2008; Seymour et al., 2012), and temporal discounting (Doya, 2002; Miyazaki et al., 2011). Although it is known that DR and MR project to overlapping, yet distinct forebrain structures (Azmitia and Segal, 1978; Vertes and Linley, 2008; Vertes et al., 1999), experimental manipulations in DR and MR have yielded equivocal results, and how serotonin neurons in these areas function remains elusive.

Forebrain-projecting dopamine neurons are mainly found in the ventral tegmental area (VTA) and the substantia nigra pars compacta (SNc). Neurophysiological recordings in behaving animals have demonstrated that many putative dopamine neurons signal the discrepancy between actual and expected reward, that is, reward prediction error (Bayer and Glimcher, 2005; Matsumoto and Hikosaka, 2009; Schultz et al., 1997). Although VTA and SNc contain diverse cell types forming complex circuits, recent studies have clarified the regulation and functional roles of dopamine neurons (Cohen et al., 2012; Lammel et al., 2012; Steinberg et al., 2013; Tan et al., 2012; Tsai et al., 2009; van Zessen et al., 2012). Furthermore, monosynaptic inputs to dopamine neurons in VTA and SNc were identified from the whole brain using a rabies-virus-based transsynaptic tracing method (Watabe-Uchida et al., 2012). These studies have provided a foundation of our understanding of the anatomy and physiology of dopamine neurons as well as their diversity (Lammel et al., 2013; Roeper, 2013).

Compared to dopamine, our understanding of serotonin has been limited. One reason is that DR and MR contain a diverse collection of cell types (Hioki et al., 2010). It has thus been difficult to identify serotonin neurons while recording in behaving animals (Allers and Sharp, 2003; Kocsis et al., 2006; Nakamura et al., 2008; Ranade and Mainen, 2009). Furthermore, although previous studies identified afferents to the DR and MR (Aghajanian and Wang, 1977; Gervasoni et al., 2000; Marcinkiewicz et al., 1989; Peyron et al., 1998; Soiza-Reilly and Commons, 2011; Vertes and Linley, 2008), technical limitations of conventional tracers have made it difficult to distinguish between synaptic inputs to serotonin versus nonserotonin neurons.

To understand the organizing principles of afferents to serotonin neurons, we applied a rabies-virus-based tracing method (Watabe-Uchida et al., 2012; Wickersham et al., 2007) to identify

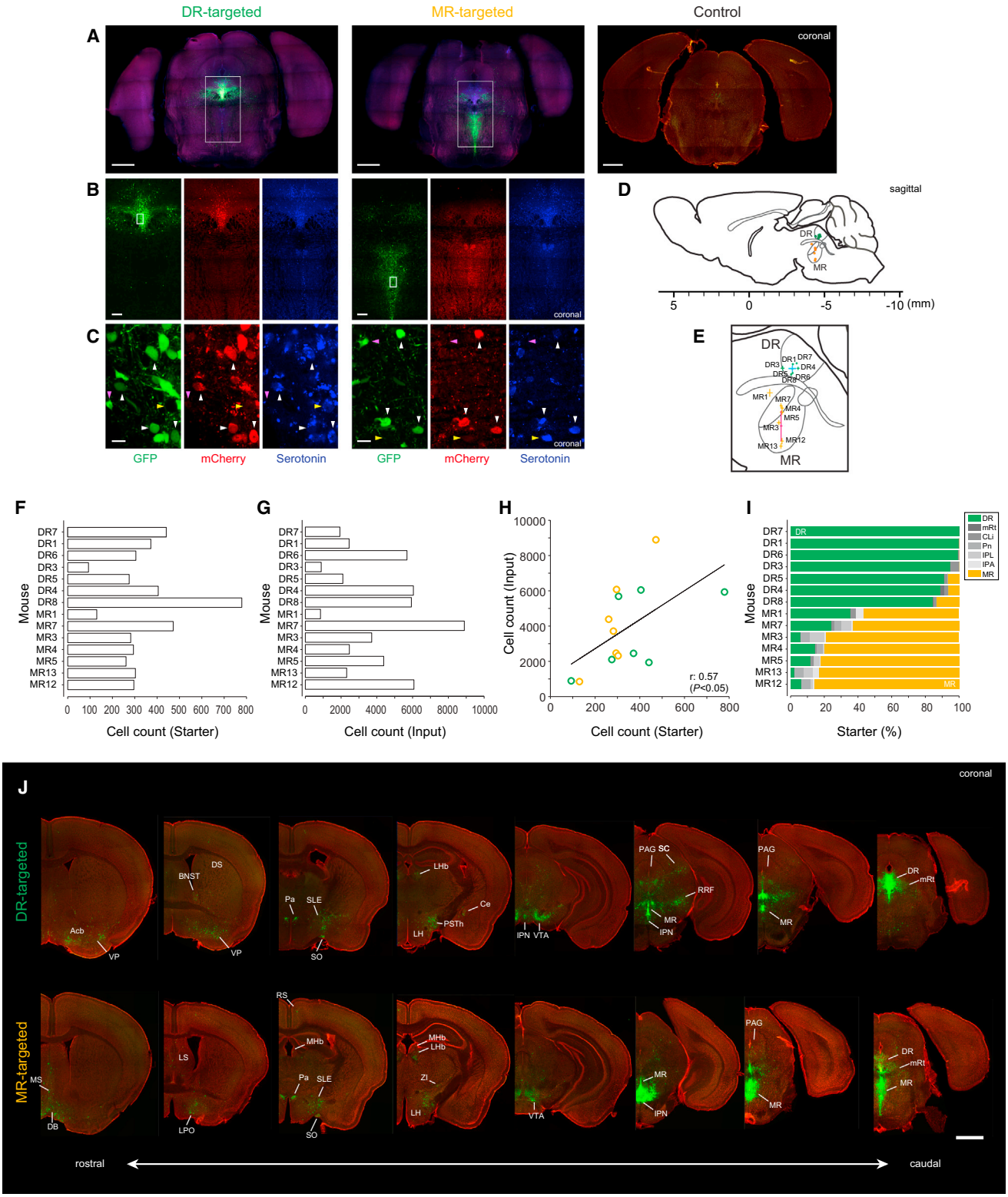

Figure 1. Identification of Monosynaptic Inputs to Serotonin Neurons with Rabies Virus and *Sert*-Cre Mice

(A–C) Injection site in the raphe nuclei of DR-targeted and MR-targeted *Sert*-Cre mice brains in low- (A), middle- (B), and high-magnification images (C). Bregma: −4.65 mm. The EGFP expression and immunoreactivity to mCherry and serotonin are shown in green, red, and blue, respectively. The white rectangles indicate the magnified regions. White arrowheads point at neurons that are triple-positive for EGFP, mCherry, and serotonin (starter neurons that are serotonergic), and

(legend continued on next page)

monosynaptic inputs to DR and MR serotonin neurons throughout the brain. We then compared the distributions of inputs to DR and MR serotonin neurons.

In addition, dopamine and serotonin are thought to be involved in related functions such as processing reward and punishment and are thought to interact (Boureau and Dayan, 2011; Kapur and Remington, 1996). However, little is known about the anatomical basis of these interactions. We therefore compared the data obtained for serotonin with those obtained for dopamine neurons in a previous study (Watabe-Uchida et al., 2012). These results provide foundational information as to the global organization of monosynaptic inputs to subdivisions of the serotonin and dopamine systems.

RESULTS

Whole-Brain Mapping of Monosynaptic Inputs to Serotonin Neurons

To demonstrate monosynaptic inputs to DR and MR serotonin neurons, we used a retrograde transsynaptic tracing system based on a modified rabies virus (SADΔG-EGFP(EnvA); Wickersham et al., 2007). This virus is pseudotyped with an avian virus envelope protein (EnvA), so that, in mammalian brains, initial infection is restricted to cells that are engineered to express a cognate receptor (TVA protein). In addition, this rabies virus lacks the gene encoding the rabies virus envelope glycoprotein (RG), which is required for transsynaptic spread. This allows for the restriction of transsynaptic spread only from cells that exogenously express RG (thus, only mono-, but not polysynaptic, inputs are labeled). To express TVA and RG in serotonin neurons, we injected two helper viruses that express TVA and RG under the control of Cre recombinase (AAV5-FLEX-TVA-mCherry and AAV8-FLEX-RG; Watabe-Uchida et al., 2012) into mice expressing Cre specifically in serotonin neurons (*Sert*-Cre mice; Zhuang et al., 2005). Injections were targeted to either DR or MR. After 14 days, we injected SADΔG-EGFP(EnvA) into the same area, and analyzed the brains 7 days later.

Here, neurons that express TVA are labeled by a red fluorescent protein, mCherry. Neurons that are infected by the rabies virus express an enhanced green fluorescent protein, EGFP. We identified starter neurons based on coexpression of mCherry and EGFP (Figures 1A–1I). Almost all double-positive neurons (95.8%) were found to be serotonin neurons (Figure 1C), by costaining of an antibody against serotonin. Near the center of injection sites, 30.5% of serotonin neurons were double positive for mCherry and EGFP. We found a small number of mCherry- and EGFP-double-positive neurons in neighboring serotonin-containing nuclei: the pontine reticular nucleus (Pn), mesencephalic reticular formation (mRt), caudal linear nucleus of the raphe (CLi), and parts of the interpeduncular nucleus (IPN). However, these neurons made up a small fraction of total starter neurons in most animals (Figure 1I). Starter neurons tiled almost the entire DR or MR (see Supplemental Experimental Procedures). Across animals, the number of EGFP-positive neurons was roughly proportional to the number of starter neurons ($Input = a \cdot Starter + b$; $a = 8.2$, $p < 0.05$; $b = 1075$, $p = 0.42$; Figures 1F–1H).

These results, together with previous studies (Miyamichi et al., 2013; Wall et al., 2013; Watabe-Uchida et al., 2012; Wickersham et al., 2007), indicate that EGFP-positive neurons outside injection sites represent transsynaptically labeled monosynaptic inputs to serotonin neurons. Because there was slight nonspecific labeling in serotonergic nuclei adjacent to injection sites, we excluded data from these areas for the following analysis. IPN is located just anterior to MR, and the caudal apical and caudal ventrolateral subnuclei of IPN (IPA and IPVL/IPL; Hale and Lowry, 2011) contain some serotonin neurons (Groenewegen and Steinbusch, 1984). IPA and IPL contained a small number of starter neurons but other IPN subnuclei did not. Therefore, we counted input neurons in IPN after excluding IPA and IPL. The following analysis uses twelve animals, seven with preferential injections into DR and five with preferential injections into MR (Figure 1I). All results reported below were further verified using the two or three animals with highest specificity for either DR or MR.

For both DR and MR serotonin neurons, EGFP-positive neurons (which we refer to as "input neurons") were distributed throughout the brain (Figure 1J). However, they were mostly found at relatively ventral portions of the forebrain and in midbrain and brainstem structures close to DR and MR. Interestingly, although DR and MR are both midline structures, inputs to DR serotonin neurons were generally more lateral than inputs to

magenta arrowheads indicate EGFP-positive but mCherry- and serotonin-negative neurons (input neurons). The yellow arrowheads point at EGFP-negative serotonergic neurons. Scale bars represent 1 mm in (A), 0.2 mm in (B), and 10 μm in (C). (A, control) Low-magnification image of the injection site (DR) in wild-type mice. Red, Nissl stain. Green, EGFP. Bregma: −4.5 mm. Scale bar represents 1 mm.

(D and E) Centers of injection sites from individual animals. Geometric means are shown by circles (D) or crosses (E, mean ± SEM). Green, DR-targeted animals; orange, MR-targeted animals. Scale bar in (D) represents distance from bregma. Cyan and magenta crosses in (E) are mean ± SEM of centers of injection sites from seven animals in DR-targeted group (DR1, DR3, DR4, DR5, DR6, DR7, and DR8) and five animals in MR-targeted group (MR3, MR4, MR5, MR12, and MR13).

(F) Numbers of starter neurons.

(G) Numbers of transsynaptically labeled neurons ("input neurons").

(H) Relationship between numbers of starter and input neurons.

(I) Proportions of labeled neurons in each of the serotonin-neuron containing nuclei. DR, dorsal raphe; mRt, mesencephalic reticular formation; CLi, caudal linear nucleus of the raphe; Pn, pontine reticular nucleus; IPL, interpeduncular nucleus lateral subnucleus; IPA, interpeduncular nucleus apical subnucleus; and MR, median raphe.

(J) Coronal sections for DR- and MR-targeted cases (DR4 and MR5, respectively). Scale bar represents 1 mm. Acb, nucleus accumbens; MS, medial septal nucleus; DB diagonal band of Broca; VP, ventral pallidum; BNST, bed nucleus of the stria terminalis; DS, dorsal striatum; LS, lateral septal nucleus; LPO, lateral preoptic area; Pa, paraventricular hypothalamic nucleus; SLE, sublenticular extended amygdala; SO, supraoptic nucleus; RS, retrosplenial cortex; MHb, medial habenula; LHb, lateral habenula; PSTh, parasubthalamic nucleus; LH, lateral hypothalamus; Ce, central amygdala nucleus; ZI, zona incerta; VTA, ventral tegmental area; IPN, interpeduncular nucleus; SC, superior colliculus; PAG, periaqueductal gray; and RRF, retrorubral field. Left to right corresponds to rostral to caudal (coordinates: Bregma, 0.7, 0.14, –0.88, –2.00, –3.28, –4.00, –4.30, and –4.60 mm).

MR serotonin neurons. This roughly matches their axonal projection patterns; MR neurons project mainly to midline structures and the hippocampus whereas DR neurons project to a broader array of regions, including more lateral areas (Azmitia and Segal, 1978; Vertes and Linley, 2008; Vertes et al., 1999).

Comparison between Inputs to DR and MR Serotonin Neurons

To quantify the distributions of monosynaptic inputs, we identified areas based on a standard mouse atlas (Franklin and Paxinos, 2008). We then registered the locations of labeled neurons to standard anatomical coordinates. To correct for variability in the total number of neurons (Figure 1G), the data were normalized by the total number of input neurons in each animal (Figures 2, S1, and S2).

We found striking differences in rostral forebrain areas, particularly in the basal ganglia and septum (Figure 2): inputs to DR serotonin neurons were distributed widely across the basal ganglia, whereas many fewer inputs to MR serotonin neurons were found there. For instance, DR serotonin neurons received many inputs from the ventral pallidum (VP), globus pallidus (GP), dorsal striatum (DS), and nucleus accumbens (Acb), although labeled neurons in the latter two structures may be "spill-over" from the VP and GP (Figures 2 and 3). That is, labeled neurons were very sparse in the center of DS and Acb, but some were found at the periphery of DS and Acb, bordering VP and GP. DR serotonin neurons also received many inputs from areas in the extended amygdala, such as the interstitial nucleus of the posterior limb of the anterior commissure (IPAC), the bed nucleus of the stria terminalis (BNST), the sublenticular extended amygdala (SLE; Figures 2 and 3), and the central nucleus of the amygdala (Ce; Figures 2 and S3). In contrast, MR serotonin neurons received very few inputs from these areas; they received inputs from more medial structures (Figure 3), such as the medial and lateral portions of the septum (mainly the medial septum, MS) and the diagonal band of Broca (DB).

We also observed many inputs in the hypothalamus. Indeed, the largest numbers of inputs from the forebrain to both DR and MR serotonin neurons came from the lateral hypothalamus (LH; Figures 2 and S3). MR serotonin neurons received more inputs from the medial and lateral preoptic areas (MPA and LPO), which are medial to the areas that contain inputs to DR, such as VP and the extended amygdala (Figure 3). Other midline structures, such as the paraventricular hypothalamic nucleus (Pa) and supramammillary nucleus (SUM), provided moderate levels of input to MR serotonin neurons, whereas DR serotonin neurons received preferential inputs from the subthalamic nucleus (STh) and the parasubthalamic nucleus (PSTh; Figures 2 and S3).

There were very few inputs from the thalamus to either MR or DR serotonin neurons. However, in the epithalamus, both the lateral and medial habenula (LHb and MHb) provided dense inputs to MR serotonin neurons, with sparser projections to DR serotonin neurons (Figures 2 and 4).

In the midbrain and brainstem, IPN, the laterodorsal tegmentum (LDTg), and Pn provided many inputs to MR, but fewer to DR. VTA, the retrorubral field (RRF), SNc, and substantia nigra pars reticulata (SNr) preferentially projected to DR versus MR serotonin neurons (Figure 2). The periaqueductal gray (PAG) projected to both DR and MR, although its ventrolateral part preferentially projected to DR serotonin neurons (Figure S3). The superior colliculus (SC), the pedunculopontine tegmental nucleus (PPTg), and mRt projected strongly to both DR and MR serotonin neurons. The parabrachial nucleus (PB) had a slight preference to DR whereas the raphe magnus nucleus (RMg) preferentially projected to MR (Figure 2).

Fewer EGFP-positive neurons were found in the neocortex (Figure 2). However, there were significant differences in the distributions of inputs to DR versus MR serotonin neurons. MR serotonin neurons received more inputs from more medial cortical areas, such as the cingulate (Cg) and retrosplenial cortices (RS), whereas DR serotonin neurons received more from the orbitofrontal cortex (in particular, its lateral part, LO) and somatosensory cortex (S; Figure 4).

To quantify the similarity in the distributions of inputs to DR and MR serotonin neurons, we calculated the correlation coefficient between the numbers of input neurons across areas (Figure 5A; $r = 0.71$, $p < 0.001$). In the scatter plot, each point represents one area, and the diagonal represents the line of unity. Areas represented by points close to the diagonal provided similar numbers of inputs to DR and MR serotonin neurons, whereas areas far from the diagonal provided distinct numbers of inputs (significant differences in red, $p < 0.05$, corrected for multiple comparisons using a Bonferroni-correction, $n = 7$ and 5 for DR and MR groups, respectively). DR serotonin neurons received significantly more inputs from RRF and VP, whereas MR serotonin neurons received more from Pn, IPN, septum, LHb, SUM, and MHb. Large common inputs came from LH, PAG, mRt, and SC.

In summary, DR and MR serotonin neurons receive inputs from largely segregated areas: MR serotonin neurons from more medial structures, often close to the midline, DR serotonin neurons from more lateral structures. LH provides many inputs to both DR and MR serotonin neurons.

Comparison between Inputs to Serotonin and Dopamine Neurons

We noticed a striking similarity in the inputs to DR serotonin neurons and inputs to VTA dopamine neurons that we obtained in a previous study (Watabe-Uchida et al., 2012). For instance, areas in the basal ganglia that were identified as major inputs to VTA dopamine neurons also provided many inputs to DR serotonin neurons.

To quantify similarities in the inputs in the four data sets (inputs to DR and MR serotonin neurons and VTA and SNc dopamine neurons), we calculated correlation coefficients for all pairs of areas (Figures 5B–5F). Correlations were higher for within-serotonin or within-dopamine comparisons (that is, larger values between inputs to DR versus MR serotonin neurons or between inputs to VTA versus SNc dopamine neurons; $r = 0.71$ and 0.65, respectively, $p < 0.001$; Figures 5A and 5B). It should be noted, however, that these pairs contained common starter neurons because viral injections resulted in some labeling of the other, nontargeted structure (Figure 1I).

In addition to these pairs, we found a remarkable similarity between inputs to DR serotonin and VTA dopamine neurons (correlation coefficient, $r = 0.59$, $p < 0.001$; Figure 5C). This correlation comes from common inputs from hypothalamus (LH, PSTh, and

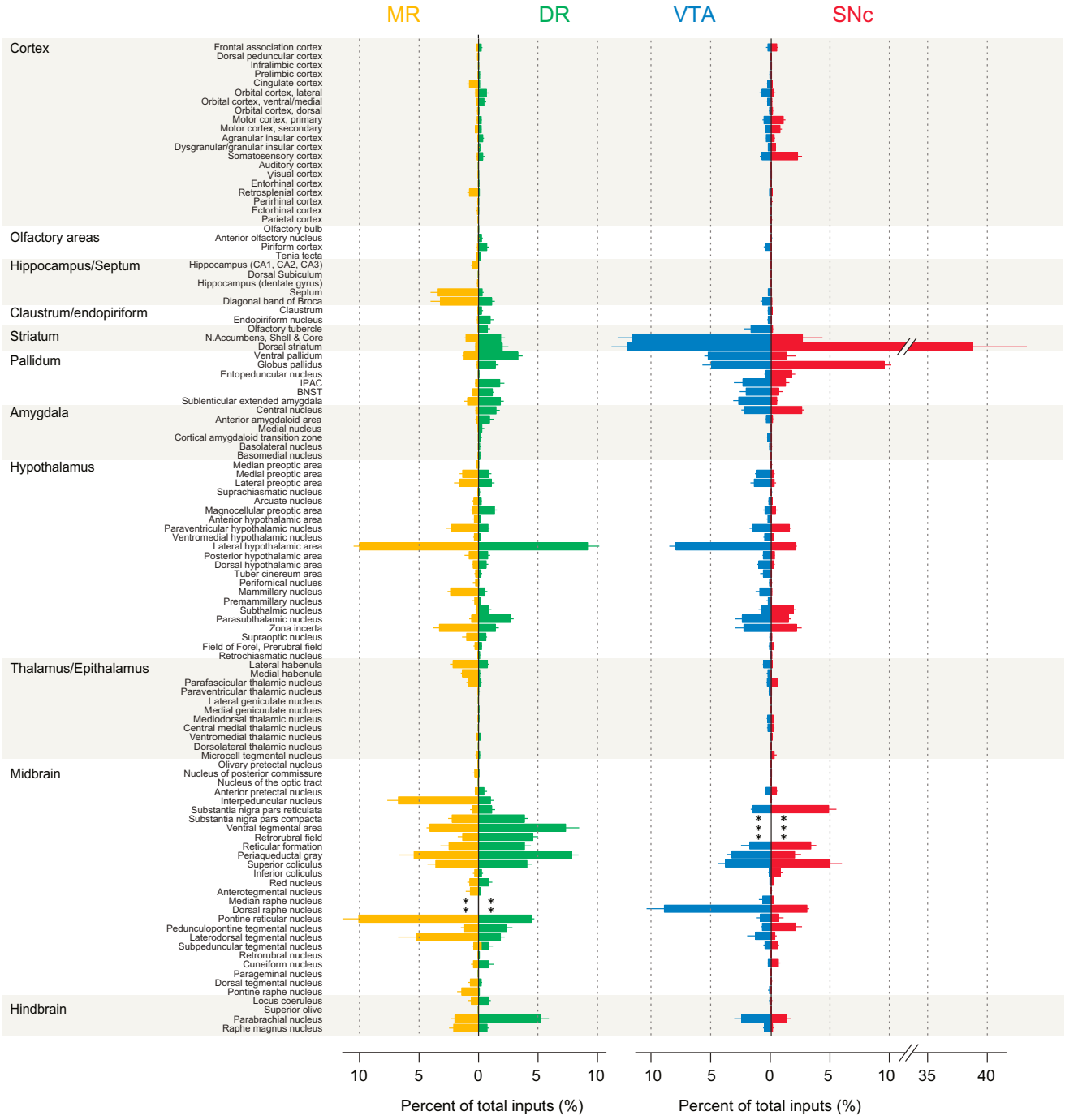

Figure 2. Summary of Monosynaptic Inputs to DR and MR Serotonin Neurons, and VTA and SNc Dopamine Neurons

(Left) Monosynaptic inputs to MR and DR serotonin neurons (orange and green, respectively). Mean ± SEM (n = 7 and 5 mice for DR and MR groups, respectively). Asterisks (*) indicate areas that are excluded from the analysis.

(Right) Monosynaptic inputs to VTA and SNc dopamine neuron (blue and red, respectively). Data from Watabe-Uchida et al. (2012).

The values are the percentage of total inputs in each area. Brain areas analyzed for MR and DR inputs are matched to the brain areas analyzed for the VTA- and SNc-targeted data set (Watabe-Uchida et al., 2012). An analysis containing a more comprehensive set of areas is shown in Figure S2.

zona incerta, ZI), extended amygdala (Ce, BNST, IPAC, and SLE), basal ganglia (VP, STh, and SNr), and other midbrain and brainstem structures (SC, PB, mRt, and LDTg). A major difference, however, existed in inputs from the striatum (Acb and DS). For VTA dopamine neurons, Acb and DS provided the largest number of inputs (Figure 2). In contrast, DR serotonin

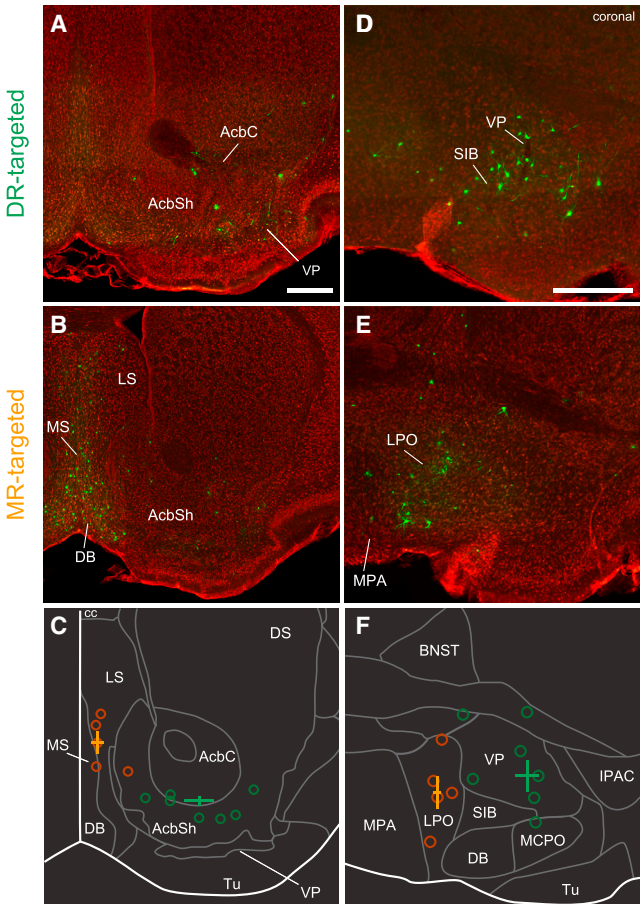

Figure 3. Spatial Shift of Input Areas for DR and MR Serotonin Neurons in the Forebrain

(A–C) Septal and striatal areas. (A) DR-targeted. (B) MR-targeted. Green, EGFP; Red, fluorescent Nissl staining. (C) The median of the coordinates of all input neurons. Open circles indicate the medians from individual animals. Crosses indicate the mean ± SEM of medians in DR- or MR-targeted groups (n = 7 and 5 mice for DR and MR groups, respectively). Green, DR targeted; orange, MR-targeted. Scale bar represents 0.5 mm. Bregma: 1.1 mm.

(D–F) Pallidal and hypothalamic areas. (D) DR-targeted. (E) MR-targeted. Same conventions as (A) through (C). Bregma: 0.14 mm.

Abbreviations as in Figure 1; AcbC, nucleus accumbens core; AcbSh, nucleus accumbens shell; cc, corpus callosum; Tu, olfactory tubercle; MPA, medial preoptic nucleus; SIB, substantia innominata basal part; MCPO, magnocellular preoptic nucleus; and IPAC, interstitial nucleus of the posterior limb of the anterior commissure.

neurons received many fewer inputs from Acb and DS. Upon removing these two areas (Acb and DS), the correlation value increased to 0.81 ($p < 0.001$). On the other hand, DR serotonin neurons received more inputs from PAG and Pn.

This high similarity between DR serotonin and VTA dopamine neurons was in contrast to low similarities between other pairs of neuron populations (Figures 5D–5F). Whereas correlations were found between inputs to DR serotonin and SNc dopamine neurons ($r = 0.21$, $p < 0.05$; Figure 5D) and between inputs to VTA dopamine and MR serotonin neurons ($r = 0.31$, $p < 0.01$; Figure 5E), inputs to SNc dopamine and MR serotonin neurons had essentially no correlation ($r = 0.02$, $p = 0.83$; Figure 5F), suggesting a gradual difference of the input patterns of MR, DR, VTA, and SNc (Figure 5G).

To compare the spatial distributions of input neurons across brains, we transformed each coronal section to match a section from a standard atlas (Franklin and Paxinos, 2008). The distributions of EGFP-labeled neurons were then compared by making horizontal slices using the morphed brains for each population of neurons (Figure S4). We also generated a flat map representation (after Swanson, 2000) to indicate the proportion of inputs to each of the four postsynaptic neuron types, conserving the rough locations in the anterior-posterior and medial-lateral axes in the forebrain (Figure 6A) and the dorsal-ventral and medial-lateral axis on a coronal section at the level of midbrain and brainstem (Figure 6B). These representations showed that (1) more medial structures (Cg, RS, Septum, DB, Pa, MHb, LHb, SUM, and IPN) projected to MR serotonin neurons; (2) intermediate structures (LO, Acb, VP, BNST, SLE, IPAC, LH, and PSTh) projected to VTA dopamine and DR serotonin neurons, although Acb did not project strongly to DR serotonin neurons; and (3) more lateral and dorsal structures (M2, M1, S, DS, GP, Ce, STh, and SNr) projected to SNc dopamine neurons. These observations show that the correlation values mentioned above correspond to spatial distributions along the medial-lateral axis.

In summary, a similar set of areas projects directly to DR serotonin and VTA dopamine neurons (Figure 5G), with the exception of the striatum. In contrast, MR serotonin neurons and SNc dopamine neurons receive different sets of inputs.

Serotonin-Dopamine Interactions

The similar inputs to VTA dopamine and DR serotonin neurons raise the possibility that these common sources similarly regulate the activity of VTA dopamine and DR serotonin neurons. In addition to these common inputs, previous studies indicated that interactions between serotonin and dopamine neurons may play an important role in behavior (Di Giovanni et al., 2010). Therefore, we examined monosynaptic connections between serotonin and dopamine neurons.

A previous study showed that VTA (and, to a lesser extent, SNc) dopamine neurons receive heavy monosynaptic inputs from DR (Watabe-Uchida et al., 2012). In contrast, both VTA and SNc dopamine neurons receive many fewer inputs from MR (Watabe-Uchida et al., 2012). Here, we examined their interactions in the opposite direction: which of the midbrain areas that contain dopamine neurons (VTA, SNc, and RRF) projects to serotonin neurons? We found that DR serotonin neurons received heavy inputs from all three areas (VTA, SNc, and RRF; Figures 7A–7F). MR serotonin neurons also received heavy inputs from VTA but fewer from SNc and RRF. Thus, DR serotonin neurons have strong reciprocal connections with both VTA and SNc whereas MR serotonin neurons have a unidirectional connection from VTA.

The reciprocal connection between DR and VTA has been reported (Geisler and Zahm, 2005; Vertes et al., 1999) but which cell types contribute to these interactions is unknown. In particular, whereas serotonergic regulation of VTA dopamine neurons was confirmed by multiple methods (Boureau and Dayan, 2011), projections from dopamine to serotonin neurons have remained

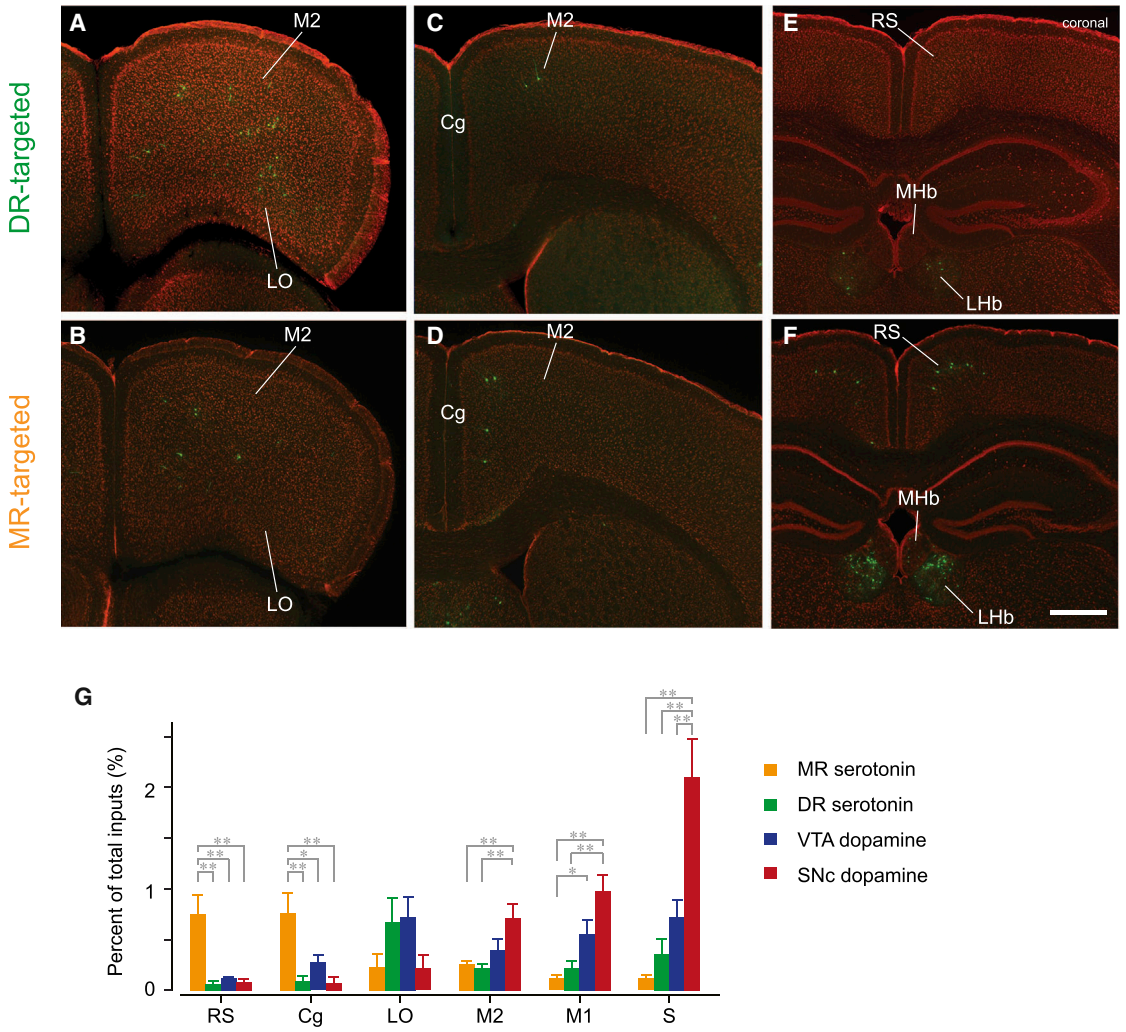

Figure 4. Monosynaptic Inputs from the Cortex and Habenula

(A–F) Distributions of input neurons to DR (A, C, and E) and MR (B, D, and F) serotonin neurons. Scale bar represents 0.5 mm. Abbreviations as in Figure 1. LO, lateral orbital cortex; M2, secondary motor cortex; Cg, cingulate cortex; and RS, retrosplenial cortex. Bregma: 2.58 mm (A and B), 0.86 mm (C and D), and −1.70 mm (E and F).

(G) Percent of total inputs in six cortical areas that contained relatively large numbers of input neurons (>0.7% in at least one of the four experimental groups). MR (orange), DR (green), VTA (blue), and SNc (red). Mean ± SEM (n = 7 and 5 mice for DR and MR groups, n = 4 mice each for VTA and SNc groups, respectively). $^{**}p < 0.01$ and $^{*}p < 0.05$, one-way ANOVA, Tukey-Kramer multiple comparison test.

unclear (Ferreira et al., 2008; Kalén et al., 1988). Our results thus far have specified postsynaptic cell types (dopamine or serotonin neurons). In the following, we examined presynaptic cell types by immunostaining in combination with transsynaptic tracing with the modified rabies virus using *Sert*-Cre mice and *DAT*-Cre mice.

We stained against tyrosine hydroxylase (TH) in sections in which monosynaptic inputs to DR serotonin neurons were labeled and against serotonin in sections in which monosynaptic inputs to VTA dopamine neurons were labeled (Figures 7G and 7H). The results showed that many monosynaptic inputs to dopamine neurons were serotonergic (54.0%; Figure 7I). In contrast, few (only 8.1%) monosynaptic inputs to serotonin neurons were dopaminergic (Figure 7I), consistent with previous observations (Kalén et al., 1988). Interestingly, VTA inputs to serotonin neurons clustered in the posterior-ventral-medial part of the SNc and in the ventral-lateral part of VTA, surrounding the medial leminiscus (Figures 7A and 7B).

Thus, inputs from DR to VTA dopamine neurons include a large number of serotonergic projections, whereas inputs from VTA (and SNc) to DR serotonin neurons do not contain many dopaminergic projections, suggesting a largely unidirectional projection from serotonin to dopamine neurons (Figure 7J).

DISCUSSION

Using a modified rabies virus, we mapped the whole-brain monosynaptic inputs to DR and MR serotonin neurons. We

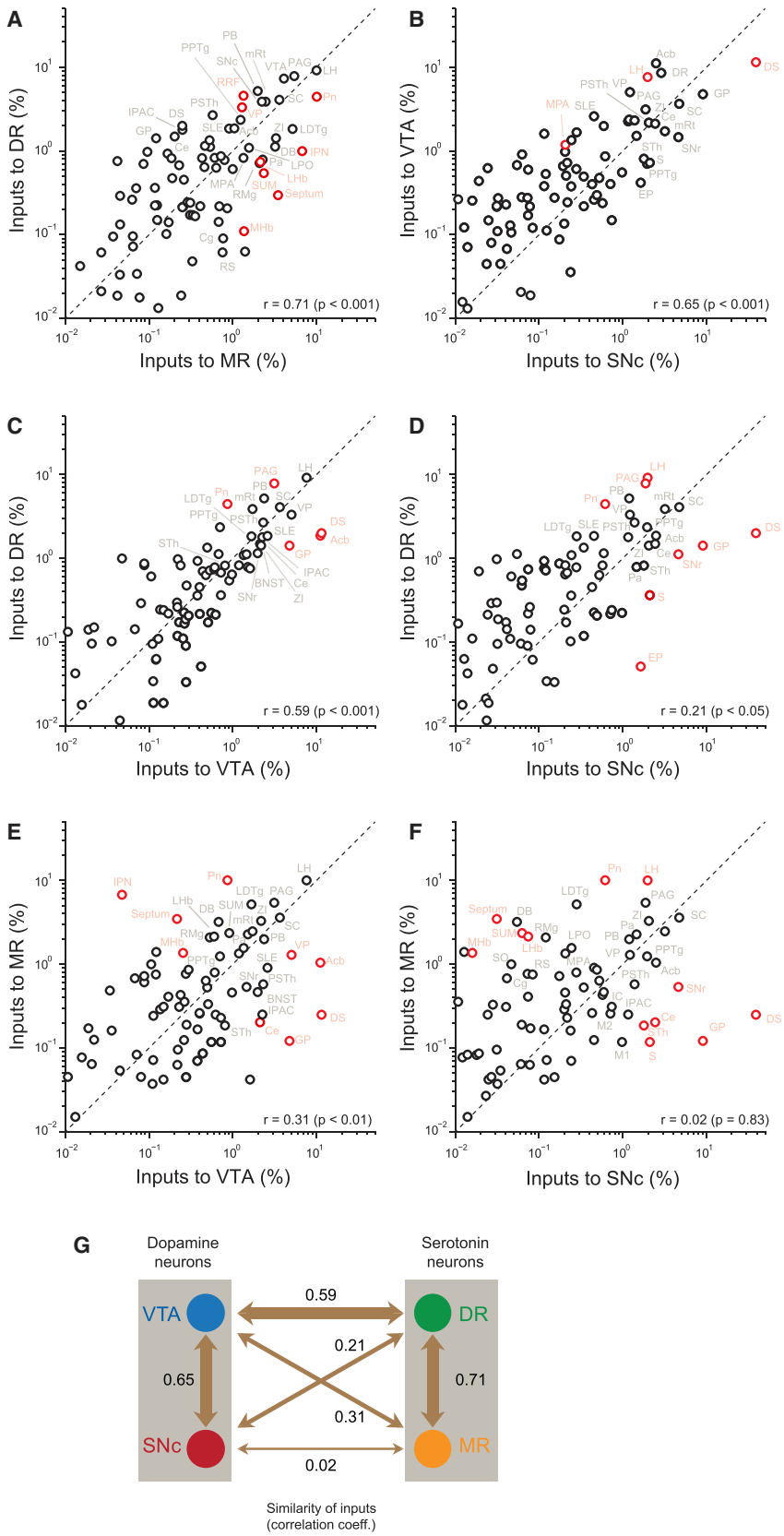

Figure 5. Comparisons of Monosynaptic Inputs across Four Groups

(A) Comparison between inputs to DR and MR serotonin neurons. (DR, n = 7 mice; MR, n = 5 mice).

(B) Comparison between inputs to VTA and SNc dopamine neurons (VTA, n = 4; SNc n = 4).

(C) Comparison between inputs to DR serotonin and VTA dopamine neurons.

(D) Comparison between inputs to DR serotonin and SNc dopamine neurons.

(E) Comparison between inputs to MR serotonin and VTA dopamine neurons.

(F) Comparison between inputs to MR serotonin and SNc dopamine neurons.

Values are the means of percent of total inputs from each region. Red circles indicate significant differences ($p < 0.05$, Bonferroni-corrected). *r*: Pearson's correlation coefficients.

(G) Summary of similarities between input patterns. Numbers indicate correlation coefficients. The thickness of each arrow indicates the similarity.

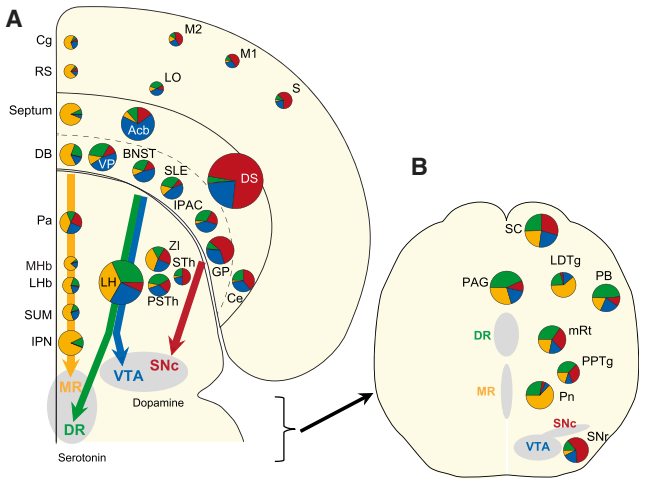

Figure 6. Three Input "Axes" for Serotonin and Dopamine

Each pie chart represents the percentage of total inputs for each postsynaptic neuron type, and are placed at their rough locations in the anterior-posterior and medial-lateral axes on a horizontal section of the forebrain (A) and the dorsal-ventral and medial-lateral axes on a coronal section at the level of midbrain and brainstem (B). Color represents postsynaptic neuron types: inputs to MR serotonin neurons (orange), DR serotonin neurons (green), VTA dopamine neurons (blue), and SNc dopamine neurons (red). The size of the pie charts reflects the sum of the percentages. Colored arrows indicate the main axes of input streams.

found that MR serotonin neurons receive inputs from more medial forebrain areas than DR serotonin neurons. We next compared the distributions of inputs to serotonin neurons with those to dopamine neurons obtained in a previous study (Watabe-Uchida et al., 2012). We found a remarkable overall similarity between inputs to VTA dopamine and DR serotonin neurons. This comparison also revealed an important difference: compared to serotonin neurons, dopamine neurons receive many more direct inputs from the striatum. These results demonstrate a global organizing principle of inputs to two major ascending neuromodulator systems. There are roughly three descending input streams: medial areas project to MR serotonin neurons, intermediate areas project to DR serotonin and VTA dopamine neurons, and more lateral areas project to SNc dopamine neurons.

Similarity between Inputs to DR Serotonin and VTA Dopamine Neurons

Comparing the relative numbers of inputs across areas, we found that DR serotonin and VTA dopamine neurons receive quantitatively similar patterns of inputs compared to MR serotonin and SNc dopamine neurons (Figure 5G). These findings notably advance the literature in two ways: first, our analysis is based on direct inputs to serotonin and dopamine neurons, a specificity that has been difficult to achieve with conventional tracers (Wickersham et al., 2007). Second, although differences in inputs to subareas of either dopamine or serotonin system have been noted qualitatively in previous studies (Graybiel and Ragsdale, 1979; Ikemoto, 2007; Vertes and Linley, 2008; Watabe-Uchida et al., 2012), our analysis is a quantitative comparison between different neurotransmitter systems (here, dopamine and serotonin).

The similarities and differences observed between inputs to DR serotonin and VTA dopamine neurons may provide insight into their functions. Serotonin has been proposed to be involved in diverse functions but it has been difficult to pinpoint any specific one. Proposed functions of serotonin partially overlap with those of dopamine, but their roles often appear opposed. For instance, dopamine is associated with positive reinforcement and promoting approach/exploration behavior, whereas serotonin is associated with negative reinforcement and behavioral inhibition (Daw et al., 2002; Dayan and Huys, 2008; Deakin and Graeff, 1991; den Ouden et al., 2013; Soubrie, 1986). This idea of opponency between the two systems has been supported by the observation that serotonin neurons are activated by noxious stimuli (Montagne-Clavel et al., 1995; Schweimer and Ungless, 2010) whereas dopamine neurons are activated by reward. It remains to be determined how these observations can be reconciled with recent studies showing that many DR neurons (which likely included serotonin neurons) were excited by reward (Miyazaki et al., 2011; Nakamura et al., 2008; Ranade and Mainen, 2009). These results suggest that the way DR serotonin neurons respond during behavior bears some similarity to that of dopamine neurons, although critical differences may exist. Our study showed that LH provided extremely dense input to DR serotonin and VTA dopamine neurons. Given that some LH neurons signal subjective values (Ono et al., 1986), it is possible that LH underlies the similarity of their responses during appetitive events.

A striking difference between inputs to DR serotonin and VTA dopamine neurons is the much smaller number of direct inputs from the striatum (Acb and DS) to DR serotonin neurons. For both VTA and SNc dopamine neurons, the largest number of inputs comes from the striatum (Watabe-Uchida et al., 2012). In contrast, DR serotonin neurons receive more inputs from pallidal/extended amygdala structures and from LH. Dopamine neurons receive inputs from the striatum both directly and indirectly through pallidal and hypothalamic structures (Watabe-Uchida et al., 2012). Our results suggest that DR serotonin neurons receive primarily indirect inputs from the striatum. It has been proposed that striatal neurons provide reward expectation signals to directly inhibit dopamine neurons to calculate reward prediction errors (Doya, 1999; Houk et al., 1995), although the functional role of this input remains to be clarified. The small number of direct inputs from the striatum to DR serotonin neurons might be related to the observation that DR serotonin neurons respond to reward even when reward is expected (Nakamura et al., 2008). In addition to the striatum, serotonin neurons do not receive inputs from other areas to which they project, such as hippocampus, thalamus, and amygdala. In contrast, dopamine neurons receive inputs from most of their projection sites (that is, they have reciprocal connections). This may explain the longer timescale responses in serotonin neurons because of the lack of immediate negative feedback as found in dopamine neurons (Haber et al., 2000).

Forebrain-Habenula-Raphe Serotonin Pathways

The habenula (Hb) has long been considered a node of major descending pathways to serotonin neurons emanating from

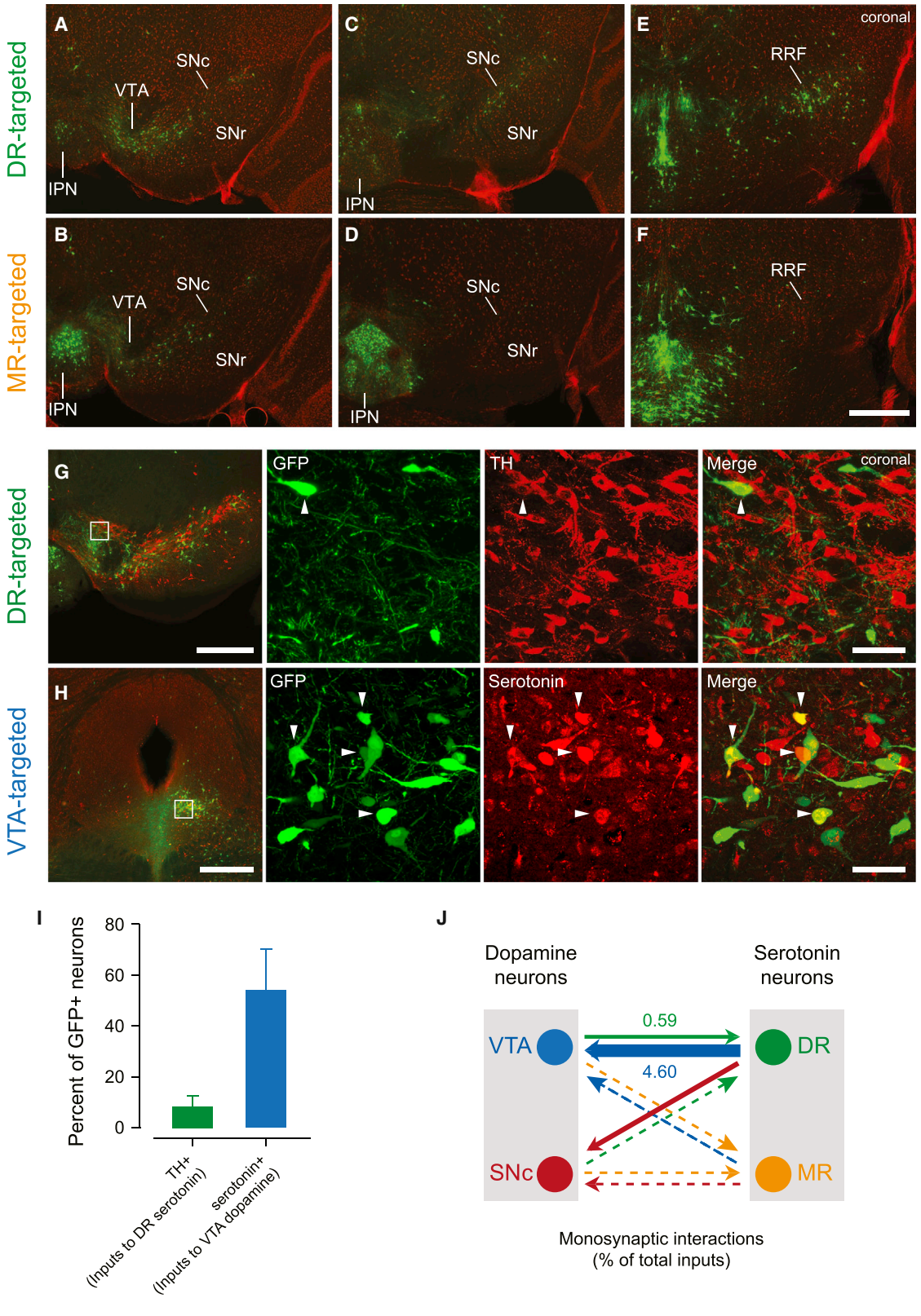

(legend on next page)

various forebrain regions. Whereas the MHb-IPN-raphe route conveys information from the hippocampal system to serotonin neurons, the LHb-raphe route conveys different kinds of information from the basal ganglia and hypothalamus to serotonin neurons (Herkenham and Nauta, 1979). We found two major differences between Hb inputs to DR versus MR serotonin neurons as described below.

We found that LHb sends strong monosynaptic inputs to MR serotonin neurons, consistent with previous findings (Behzadi et al., 1990). On the other hand, although LHb projects strongly to DR (Vertes et al., 1999), we found that DR serotonin neurons (and VTA and SNc dopamine neurons) receive few monosynaptic inputs from LHb. Recent studies found that the rostromedial tegmental nucleus (RMTg) relays inputs from LHb to DR as well as to dopamine neurons (Jhou et al., 2009). Because most LHb neurons are excitatory and RMTg neurons are inhibitory, our data suggest that activation of LHb neurons can exert opponent control over MR and DR serotonin neurons. That is, LHb neurons directly excite MR serotonin neurons and, at the same time, inhibit DR serotonin neurons (and dopamine neurons) via RMTg.

Although previous studies indicated that IPN projects to both MR and DR (Groenewegen et al., 1986), our results showed that IPN projects preferentially to MR, over DR, serotonin neurons. Most inputs originate from rostral IPN (Figures 7A–7D), which receives strong projections from MHb. We also found that MHb projects directly to MR (Figures 2 and 4F). These results show that MR serotonin neurons receive strong inputs directly and indirectly (via IPN) from MHb (Figure S5).

Previous studies found that MR receives input from extended amygdala (e.g., BNST) and basal ganglia (e.g., VP) (Marcinkiewicz et al., 1989; Vertes and Linley, 2008). However, our data showed few monosynaptic inputs from these areas to MR serotonin neurons. Recent studies showed that these areas project to RMTg, which is adjacent to MR (Jhou et al., 2009). Other studies using anterograde tracers indicated that Acb and VP project to the lateral part of MR but not to the midline where most serotonin neurons reside (Behzadi et al., 1990). These results suggest that differences between studies can be explained by the higher specificity of labeling in the present study.

Hierarchical Organization between Dopamine and Serotonin

Serotonin and dopamine systems are thought to interact (Boureau and Dayan, 2011; Kapur and Remington, 1996). Our data showed that both DR serotonin and VTA dopamine neurons receive a large number of monosynaptic inputs from VTA and DR, respectively. However, although inputs from DR to VTA dopamine neurons included many serotonin neurons, inputs from VTA (and SNc) to DR serotonin neurons did not contain many dopamine neurons. These results indicate a largely one-directional information flow from DR serotonin neurons to VTA and SNc dopamine neurons (Figure 7J).

It is interesting that, although both DR serotonin and VTA and SNc dopamine neurons project to the striatum, the striatum sends back massive projections primarily to dopamine (Watabe-Uchida et al., 2012), and not serotonin neurons (present study). Therefore, serotonin could also control dopamine neurons by regulating striatal activity (Kapur and Remington, 1996) but not vice versa. This suggests a hierarchical relationship between DR serotonin and VTA and SNc dopamine neurons; overall, serotonin is in a stronger position to control dopamine than vice versa both through direct and indirect connections. Our data match observations that lesions of DR or MR or pharmacological manipulations of serotonin affect dopamine release (Boureau and Dayan, 2011; Di Giovanni et al., 1999; Hervé et al., 1979). This serotonin-dopamine interaction is important for understanding neural circuits for reinforcement learning. It has been proposed that serotonin adds affective tone by inhibiting dopamine signals (Boureau and Dayan, 2011; Daw et al., 2002). Moreover, drugs for psychiatric disorders such as schizophrenia, depression, and addiction act directly or indirectly on both serotonin and dopamine (Kapur and Remington, 1996). The anatomical basis of serotonin-dopamine interactions analyzed in the present study can provide insight into normal reward processing as well as brain disorders.

Three Axes of Descending Control of Dopamine and Serotonin

Our data suggest that three axes of descending projections control serotonin and dopamine (Figure 6). The most medial axis originates from the septo-hippocampal system and controls MR serotonin neurons. The intermediate axis originates from the ventral basal ganglia/extended amygdala and LH and controls VTA dopamine and DR serotonin neurons. The most lateral axis originates from the dorsal part of the basal ganglia and the subthalamic nucleus and controls SNc dopamine neurons. In addition to these subcortical descending projections, we also observed direct projections from the neocortex that follow similar segregation: somatosensory and motor cortices to SNc

Figure 7. Interactions between Serotonin and Dopamine Neurons

(A–F) Distributions of input neurons to DR (A, C, and E) and MR (B, D, and F) serotonin neurons. Abbreviations as in Figure 1; SNr, substantia nigra pars reticulata. Scale bar represents 0.5 mm. Bregma: −3.40 mm (A and B), −3.64 mm (C and D), and −4.04 mm (E and F).

(G) Monosynaptic inputs to DR serotonin neurons stained against tyrosine hydroxylase (TH). White square indicates the location of the high-magnification view on the right. White arrowhead indicates a TH-positive input neuron. Scale bars represent 0.5 mm and 50 μm (low and high-magnification images). Bregma: −3.52 mm.

(H) Monosynaptic inputs to VTA dopamine neurons stained against serotonin. White arrowheads indicate serotonin-positive input neurons. Bregma: −4.72 mm.

(I) Percentage of dopamine (among all VTA and SNc inputs) or serotonin (among all DR inputs) neurons in EGFP positive neurons. Mean ± SEM (n = 39 ± 15, 54 ± 4 neurons, and n = 2 animals each).

(J) Summary of monosynaptic connections between serotonin and dopamine neurons. Numbers indicate percent of total inputs that are serotonergic or dopaminergic, estimated by multiplying the percent of inputs from each area by the percent of dopamine- or serotonin positive-neurons among EGFP-labeled neurons. Arrow thickness reflects the number of connections. Dotted lines indicate weak (<0.5%) connections.

dopamine neurons, orbitofrontal cortex to VTA dopamine and DR serotonin neurons and medial cortical areas such as the Cg and RS to MR serotonin neurons (Figure 4G).

In this study, we observed global afferent control for serotonin and dopamine systems. Our results demonstrate that three parallel pathways form largely segregated control systems for these two neuromodulators. Across and within these pathways, DR serotonin neurons appear to exert hierarchically greater control over VTA and SNc dopamine neurons than vice versa. We compared serotonin and dopamine systems because they are thought to interact. Similar comparisons with other neuromodulators may provide insight into the global organization of brain connectivity.

EXPERIMENTAL PROCEDURES

Viral Injections

We used 14 adult (2–6 months old) female *Sert*-Cre mice (Slc6a4tm1(cre)Xz; Zhuang et al., 2005) that express Cre recombinase under the transcriptional control of the serotonin transporter gene. These mice were backcrossed with C57BL/6J mice. For some control experiments, C57BL6 mice were used. All procedures were in accordance with Harvard University Institutional Animal Care and Use Committee.

To demonstrate monosynaptic inputs to DR and MR serotonin neurons, we used a transsynaptic tracing system based on the modified rabies virus (Watabe-Uchida et al., 2012; Wickersham et al., 2007). First, 0.3–0.5 μl of AAV8-FLEX-RG (2×10^{12} particles/ml) and 0.3–0.5 μl AAV5-FLEX-TVA-mCherry (4×10^{12} particles/ml) were stereotaxically injected into the DR or MR (4.5 mm and 4.2 mm posterior to the bregma, 0 mm and 0 mm to the midline, and 2.1 mm and 3.6 mm ventral to the dura, respectively) using a micromanipulator with a pulled glass needle. Fourteen days later, 0.8–1 μl of pseudotyped rabies virus, SADΔG-EGFP(EnvA) (5×10^7 plaque-forming units [pfu] per milliliter; Wickersham et al., 2007) was injected into the same area. All surgeries were performed under aseptic conditions with animals under ketamine/medetomidine (60 and 0.5 mg/kg, intraperitoneally [i.p.], respectively) or isoflurane (1%–3% at 600 ml/min) anesthesia. Analgesia (ketofen 5 mg/kg, i.p., buprenorphine, 0.1 mg/kg, i.p.) was administered postoperatively. The data for monosynaptic inputs to VTA and SNc dopamine neurons were obtained using a similar method using *DAT*-Cre mice (Watabe-Uchida et al., 2012).

Histology

One week after injection of rabies virus, mice were perfused with PBS followed by 4% paraformaldehyde (PFA) in PBS. After 1 day of postfixation in 4% PFA, 100-μm-thick coronal slices were prepared using a vibratome. Every third section was counterstained with NeuroTrace Fluorescent Nissl Stains (Molecular Probes). To identify starter neurons infected by the rabies virus, immunohistochemistry was performed. TVA-mCherry signal was detected using either anti-mCherry mouse monoclonal antibody (1:100; Clontech) or anti-DsRed rabbit polyclonal antibody (1:200; Rockland Immunochemicals), with Alexa Fluor 594 goat anti-mouse secondary antibody, or Alexa Fluor 555 goat anti-rabbit secondary antibody (1:200; Molecular Probes). Serotonin neurons were identified using an antiserotonin rabbit polyclonal antibody (1:200; Sigma-Aldrich), or antiserotonin rat monoclonal antibody (1:100; Millipore), with biotinylated goat anti-rabbit secondary antibody (1:200; Jackson ImmunoResearch), streptavidin-conjugated Alexa Fluor 405, or Alexa Fluor 633 goat anti-rat secondary antibody (1:200; Molecular Probes). Slices were permeabilized with 0.5% Triton X-100, and incubation with antibodies and washing was done with 0.05% Triton X-100. Whole-section mosaics of low-magnification images were taken semiautomatically with AxioImager Z2, Axio Scan Z1, or LSM 700 Inverted Confocal microscope (Zeiss), and assembled using software (Axiovision or Zen, Zeiss). High-magnification images were taken by an LSM 510 or LSM 700 inverted confocal microscope (Zeiss). Starter neurons were identified based on coexpression of EGFP and mCherry (Figures 1C, 1F, and 1I).

For identification of cell types of rabies-infected neurons, we used antiserotonin and anti-TH rabbit polyclonal (1:200; Millipore) antibodies. We performed the following control experiments to quantify the specificity of these antibodies. We first crossed *Sert*-Cre and *DAT*-Cre mice (B6.SJLSlc6a3$^{tm1.1(cre)Bkmn}$/J, Jackson Lab; Bäckman et al., 2006) with tdTomato-reporter mice (Gt(ROSA)26 $^{Sortm9(CAG-tdTomato)Hze}$, Jackson Laboratory) to express tdTomato in serotonin and dopamine neurons, respectively. After fixation in 4% PFA/PBS and slicing, immunohistochemistry was performed. In *Sert*-Cre/tdTomato brain slices, 90.75 ± 4.2% (mean ± SEM, n = 3 animals) of tdTomato-positive neurons were labeled with the antiserotonin antibody. In *DAT*-Cre/tdTomato brain slices, 95.7 ± 3.2% (mean ± SEM, n = 2 animals) of tdTomato-positive neurons were labeled with anti-TH antibody.

To quantify the specificity of initial infection of starter neurons by the rabies virus, AAV5-FLEX-TVA-mCherry and pseudotyped rabies virus, SADΔG-EGFP(EnvA), were injected without AAV8-FLEX-RG into DR of *Sert*-Cre mice. Immunohistochemistry using the anti-serotonin antibody showed that 90.77 ± 1.9% (mean ± SEM, n = 3 animals) of EGFP-positive neurons were labeled by the antiserotonin antibody, which is close to the efficiency at which the antibody can label serotonin neurons.

Image Analysis

The locations of labeled neurons and the outlines of brain areas were manually registered using custom software written in MATLAB (Mathworks) and R (http://www.r-project.org/). Nomenclature, abbreviations, and outlines of brain areas are according to a standard atlas (Franklin and Paxinos, 2008). Starter and input neurons in Figures 1F–1H were counted from both hemispheres, but other data for quantitative analysis were from one hemisphere. Centers of injection sites were calculated as the arithmetic mean of the coordinates of EGFP- and mCherry-double-positive neurons in each animal. Positions of neurons were measured using the center of the aqueduct as the landmark in each brain slice.

For quantitative comparisons of input neurons between DR and MR, we used seven brains from the DR group and five brains from the MR group that contained relatively large numbers of starter neurons and transsynaptically labeled neurons, and that had highest specificities of starter neurons (DR1, DR3, DR4, DR5, DR6, DR7, and DR8; and MR3, MR4, MR5, MR12 and MR13; Figure 1I). The numbers of input neurons were normalized by the total number of inputs (excluding the injection sites) in each animal to obtain the percentage of total inputs. Because the data for inputs to dopamine neurons were based on brain areas anterior to bregma −5.34 mm (Watabe-Uchida et al., 2012), for the main analyses, we used data from the corresponding areas for inputs to serotonin as well. Analyses including more caudal areas are shown in Figure S2. The data for monosynaptic inputs to VTA and SNc dopamine neurons were reported previously (Watabe-Uchida et al., 2012). The four brains from VTA and SNc groups that were used in the previous report were also used for the analysis here (VTA: v001, v004, v009, and v010; SNc: s001, s003, s004, and s006).

To compare distributions of input neurons in the forebrain (Figure 3), the median of the coordinates of input neurons except those in the cortex was obtained. To superimpose results from different animals onto a standard atlas, positions of neurons were normalized by three landmarks: the corpus callosum at the midline, the most ventral part of the midline, and the most lateral part of the dorsal striatum.

For statistical analysis of cortical inputs (Figure 4G), multiple group comparisons were assessed with a one-way ANOVA followed by post hoc Tukey-Kramer tests.

For statistical comparisons of the number of inputs between the different starter groups (Figure 5), areas that contained <1% of the total inputs in both of the starter groups were excluded. Corrections for multiple comparisons were performed using Bonferroni corrections based on the number of all of these areas used for statistical comparisons. To quantify the similarity in input patterns, we calculated Pearson's correlation coefficients without excluding any area.

SUPPLEMENTAL INFORMATION

Supplemental Information for this article includes Supplemental Experimental Procedures and five figures and can be found with this article online at http://dx.doi.org/10.1016/j.celrep.2014.06.042.

AUTHOR CONTRIBUTIONS

S.K.O., J.Y.C., N.U., and M.W.-U. designed experiments, analyzed data, and wrote the paper. S.K.O., D.H., and M.W.-U. collected data.

ACKNOWLEDGMENTS

We are grateful to Dr. E. Callaway for providing us with the rabies virus and other reagents. We thank Drs. J.A.T. Young for pCMMP-TVA950, X. Zhuang for the *Sert*-Cre mouse, and C. Dulac for support and reagents. We thank Drs. K. Commons, S. Ikemoto, and D. Wang for critical comments on the manuscript and N. Eshel, W. Menegas, and other members of the M.W.-U. lab for discussion. This work was supported by a Howard Hughes Medical Institute Fellowship from the Helen Hay Whitney Foundation (to J.Y.C.), a Howard Hughes Medical Institute Collaborative Innovation Award (to N.U.), and NIH (R01MH095953 and R01MH101207 to N.U.).

Received: December 19, 2013
Revised: May 20, 2014
Accepted: June 20, 2014
Published: August 7, 2014

REFERENCES

Aghajanian, G.K., and Wang, R.Y. (1977). Habenular and other midbrain raphe afferents demonstrated by a modified retrograde tracing technique. Brain Res. *122*, 229–242.

Allers, K.A., and Sharp, T. (2003). Neurochemical and anatomical identification of fast- and slow-firing neurones in the rat dorsal raphe nucleus using juxtacellular labelling methods *in vivo*. Neuroscience *122*, 193–204.

Azmitia, E.C., and Segal, M. (1978). An autoradiographic analysis of the differential ascending projections of the dorsal and median raphe nuclei in the rat. J. Comp. Neurol. *179*, 641–667.

Bäckman, C.M., Malik, N., Zhang, Y., Shan, L., Grinberg, A., Hoffer, B.J., Westphal, H., and Tomac, A.C. (2006). Characterization of a mouse strain expressing Cre recombinase from the 3′ untranslated region of the dopamine transporter locus. Genesis *44*, 383–390.

Bayer, H.M., and Glimcher, P.W. (2005). Midbrain dopamine neurons encode a quantitative reward prediction error signal. Neuron *47*, 129–141.

Behzadi, G., Kalén, P., Parvopassu, F., and Wiklund, L. (1990). Afferents to the median raphe nucleus of the rat: retrograde cholera toxin and wheat germ conjugated horseradish peroxidase tracing, and selective D-[3H]aspartate labelling of possible excitatory amino acid inputs. Neuroscience *37*, 77–100.

Boureau, Y.-L., and Dayan, P. (2011). Opponency revisited: competition and cooperation between dopamine and serotonin. Neuropsychopharmacology *36*, 74–97.

Cohen, J.Y., Haesler, S., Vong, L., Lowell, B.B., and Uchida, N. (2012). Neuron-type-specific signals for reward and punishment in the ventral tegmental area. Nature *482*, 85–88.

Daw, N.D., Kakade, S., and Dayan, P. (2002). Opponent interactions between serotonin and dopamine. Neural Netw. *15*, 603–616.

Dayan, P., and Huys, Q.J.M. (2008). Serotonin, inhibition, and negative mood. PLoS Comput. Biol. *4*, e4.

Deakin, J.F., and Graeff, F.G. (1991). 5-HT and mechanisms of defence. J. Psychopharmacol. (Oxford) *5*, 305–315.

den Ouden, H.E.M., Daw, N.D., Fernandez, G., Elshout, J.A., Rijpkema, M., Hoogman, M., Franke, B., and Cools, R. (2013). Dissociable effects of dopamine and serotonin on reversal learning. Neuron *80*, 1090–1100.

Di Giovanni, G., De Deurwaerdére, P., Di Mascio, M., Di Matteo, V., Esposito, E., and Spampinato, U. (1999). Selective blockade of serotonin-2C/2B receptors enhances mesolimbic and mesostriatal dopaminergic function: a combined in vivo electrophysiological and microdialysis study. Neuroscience *91*, 587–597.

Di Giovanni, G., Esposito, E., and Di Matteo, V. (2010). Role of serotonin in central dopamine dysfunction. CNS Neurosci. Ther. *16*, 179–194.

Doya, K. (1999). What are the computations of the cerebellum, the basal ganglia and the cerebral cortex? Neural Netw. *12*, 961–974.

Doya, K. (2002). Metalearning and neuromodulation. Neural Netw. *15*, 495–506.

Ferreira, J.G.P., Del-Fava, F., Hasue, R.H., and Shammah-Lagnado, S.J. (2008). Organization of ventral tegmental area projections to the ventral tegmental area-nigral complex in the rat. Neuroscience *153*, 196–213.

Franklin, K.B., and Paxinos, G. (2008). The mouse brain in stereotaxic coordinates (Elsevier Academic Press San Diego).

Geisler, S., and Zahm, D.S. (2005). Afferents of the ventral tegmental area in the rat-anatomical substratum for integrative functions. J. Comp. Neurol. *490*, 270–294.

Gervasoni, D., Peyron, C., Rampon, C., Barbagli, B., Chouvet, G., Urbain, N., Fort, P., and Luppi, P.H. (2000). Role and origin of the GABAergic innervation of dorsal raphe serotonergic neurons. J. Neurosci. *20*, 4217–4225.

Graybiel, A.M., and Ragsdale, C.W., Jr. (1979). Fiber connections of the basal ganglia. Prog. Brain Res. *51*, 237–283.

Groenewegen, H.J., and Steinbusch, H.W. (1984). Serotonergic and non-serotonergic projections from the interpeduncular nucleus to the ventral hippocampus in the rat. Neurosci. Lett. *51*, 19–24.

Groenewegen, H.J., Ahlenius, S., Haber, S.N., Kowall, N.W., and Nauta, W.J.H. (1986). Cytoarchitecture, fiber connections, and some histochemical aspects of the interpeduncular nucleus in the rat. J. Comp. Neurol. *249*, 65–102.

Haber, S.N., Fudge, J.L., and McFarland, N.R. (2000). Striatonigrostriatal pathways in primates form an ascending spiral from the shell to the dorsolateral striatum. J. Neurosci. *20*, 2369–2382.

Hale, M.W., and Lowry, C.A. (2011). Functional topography of midbrain and pontine serotonergic systems: implications for synaptic regulation of serotonergic circuits. Psychopharmacology (Berl.) *213*, 243–264.

Herkenham, M., and Nauta, W.J.H. (1979). Efferent connections of the habenular nuclei in the rat. J. Comp. Neurol. *187*, 19–47.

Hervé, D., Simon, H., Blanc, G., Lisoprawski, A., Le Moal, M., Glowinski, J., and Tassin, J.P. (1979). Increased utilization of dopamine in the nucleus accumbens but not in the cerebral cortex after dorsal raphe lesion in the rat. Neurosci. Lett. *15*, 127–133.

Hioki, H., Nakamura, H., Ma, Y.-F., Konno, M., Hayakawa, T., Nakamura, K.C., Fujiyama, F., and Kaneko, T. (2010). Vesicular glutamate transporter 3-expressing nonserotonergic projection neurons constitute a subregion in the rat midbrain raphe nuclei. J. Comp. Neurol. *518*, 668–686.

Houk, J.C., Adams, J.L., and Barto, A.G. (1995). A model of how the basal ganglia generate and use neural signals that predict reinforcement. In Models of Information Processing in the Basal Ganglia, J.C. Houk, J.L. Davis, and G. Beiser, eds. (Cambridge, MA: MIT Press), pp. 249–270.

Ikemoto, S. (2007). Dopamine reward circuitry: two projection systems from the ventral midbrain to the nucleus accumbens-olfactory tubercle complex. Brain Res. Brain Res. Rev. *56*, 27–78.

Jacobs, B.L., and Azmitia, E.C. (1992). Structure and function of the brain serotonin system. Physiol. Rev. *72*, 165–229.

Jacobs, B.L., and Fornal, C.A. (1997). Serotonin and motor activity. Curr. Opin. Neurobiol. *7*, 820–825.

Jhou, T.C., Fields, H.L., Baxter, M.G., Saper, C.B., and Holland, P.C. (2009). The rostromedial tegmental nucleus (RMTg), a GABAergic afferent to midbrain dopamine neurons, encodes aversive stimuli and inhibits motor responses. Neuron *61*, 786–800.

Kalén, P., Skagerberg, G., and Lindvall, O. (1988). Projections from the ventral tegmental area and mesencephalic raphe to the dorsal raphe nucleus in the rat. Evidence for a minor dopaminergic component. Exp. Brain Res. *73*, 69–77.

Kapur, S., and Remington, G. (1996). Serotonin-dopamine interaction and its relevance to schizophrenia. Am. J. Psychiatry *153*, 466–476.

Kocsis, B., Varga, V., Dahan, L., and Sik, A. (2006). Serotonergic neuron diversity: identification of raphe neurons with discharges time-locked to the hippocampal theta rhythm. Proc. Natl. Acad. Sci. USA *103*, 1059–1064.

Lammel, S., Lim, B.K., Ran, C., Huang, K.W., Betley, M.J., Tye, K.M., Deisseroth, K., and Malenka, R.C. (2012). Input-specific control of reward and aversion in the ventral tegmental area. Nature *491*, 212–217.

Lammel, S., Lim, B.K., and Malenka, R.C. (2013). Reward and aversion in a heterogeneous midbrain dopamine system. Neuropharmacology.

Lydic, R., McCarley, R.W., and Hobson, J.A. (1983). The time-course of dorsal raphe discharge, PGO waves, and muscle tone averaged across multiple sleep cycles. Brain Res. *274*, 365–370.

Marcinkiewicz, M., Morcos, R., and Chrétien, M. (1989). CNS connections with the median raphe nucleus: retrograde tracing with WGA-apoHRP-Gold complex in the rat. J. Comp. Neurol. *289*, 11–35.

Matsumoto, M., and Hikosaka, O. (2009). Two types of dopamine neuron distinctly convey positive and negative motivational signals. Nature *459*, 837–841.

McGinty, D.J., and Harper, R.M. (1976). Dorsal raphe neurons: depression of firing during sleep in cats. Brain Res. *101*, 569–575.

Miyamichi, K., Shlomai-Fuchs, Y., Shu, M., Weissbourd, B.C., Luo, L., and Mizrahi, A. (2013). Dissecting local circuits: parvalbumin interneurons underlie broad feedback control of olfactory bulb output. Neuron *80*, 1232–1245.

Miyazaki, K., Miyazaki, K.W., and Doya, K. (2011). Activation of dorsal raphe serotonin neurons underlies waiting for delayed rewards. J. Neurosci. *31*, 469–479.

Montagne-Clavel, J., Oliveras, J.L., and Martin, G. (1995). Single-unit recordings at dorsal raphe nucleus in the awake-anesthetized rat: spontaneous activity and responses to cutaneous innocuous and noxious stimulations. Pain *60*, 303–310.

Nakamura, K., Matsumoto, M., and Hikosaka, O. (2008). Reward-dependent modulation of neuronal activity in the primate dorsal raphe nucleus. J. Neurosci. *28*, 5331–5343.

Ono, T., Nakamura, K., Nishijo, H., and Fukuda, M. (1986). Hypothalamic neuron involvement in integration of reward, aversion, and cue signals. J. Neurophysiol. *56*, 63–79.

Peyron, C., Petit, J.M., Rampon, C., Jouvet, M., and Luppi, P.H. (1998). Forebrain afferents to the rat dorsal raphe nucleus demonstrated by retrograde and anterograde tracing methods. Neuroscience *82*, 443–468.

Ranade, S.P., and Mainen, Z.F. (2009). Transient firing of dorsal raphe neurons encodes diverse and specific sensory, motor, and reward events. J. Neurophysiol. *102*, 3026–3037.

Roeper, J. (2013). Dissecting the diversity of midbrain dopamine neurons. Trends Neurosci. *36*, 336–342.

Schultz, W., Dayan, P., and Montague, P.R. (1997). A neural substrate of prediction and reward. Science *275*, 1593–1599.

Schweimer, J.V., and Ungless, M.A. (2010). Phasic responses in dorsal raphe serotonin neurons to noxious stimuli. Neuroscience *171*, 1209–1215.

Seymour, B., Daw, N.D., Roiser, J.P., Dayan, P., and Dolan, R. (2012). Serotonin selectively modulates reward value in human decision-making. J. Neurosci. *32*, 5833–5842.

Soiza-Reilly, M., and Commons, K.G. (2011). Glutamatergic drive of the dorsal raphe nucleus. J. Chem. Neuroanat. *41*, 247–255.

Soubrie, P. (1986). Reconciling the role of central serotonin neurons in human and animal behavior. Behav. Brain Sci. *9*, 319–364.

Steinberg, E.E., Keiflin, R., Boivin, J.R., Witten, I.B., Deisseroth, K., and Janak, P.H. (2013). A causal link between prediction errors, dopamine neurons and learning. Nat. Neurosci. *16*, 966–973.

Swanson, L.W. (2000). Cerebral hemisphere regulation of motivated behavior. Brain Res. *886*, 113–164.

Tan, K.R., Yvon, C., Turiault, M., Mirzabekov, J.J., Doehner, J., Labouèbe, G., Deisseroth, K., Tye, K.M., and Lüscher, C. (2012). GABA neurons of the VTA drive conditioned place aversion. Neuron *73*, 1173–1183.

Tsai, H.-C., Zhang, F., Adamantidis, A., Stuber, G.D., Bonci, A., de Lecea, L., and Deisseroth, K. (2009). Phasic firing in dopaminergic neurons is sufficient for behavioral conditioning. Science *324*, 1080–1084.

van Zessen, R., Phillips, J.L., Budygin, E.A., and Stuber, G.D. (2012). Activation of VTA GABA neurons disrupts reward consumption. Neuron *73*, 1184–1194.

Vertes, R.P., and Linley, S.B. (2008). Efferent and afferent connections of the dorsal and median raphe nuclei in the rat. In Serotonin and Sleep: Molecular, Functional and Clinical Aspects, J.M. Monti, S.R. Pandi-Perumal, B.L. Jacobs, and D.J. Nutt, eds. (Basel: Birkhäuser Basel), pp. 69–102.

Vertes, R.P., Fortin, W.J., and Crane, A.M. (1999). Projections of the median raphe nucleus in the rat. J. Comp. Neurol. *407*, 555–582.

Wall, N.R., De La Parra, M., Callaway, E.M., and Kreitzer, A.C. (2013). Differential innervation of direct- and indirect-pathway striatal projection neurons. Neuron *79*, 347–360.

Watabe-Uchida, M., Zhu, L., Ogawa, S.K., Vamanrao, A., and Uchida, N. (2012). Whole-brain mapping of direct inputs to midbrain dopamine neurons. Neuron *74*, 858–873.

Wickersham, I.R., Lyon, D.C., Barnard, R.J.O., Mori, T., Finke, S., Conzelmann, K.-K., Young, J.A.T., and Callaway, E.M. (2007). Monosynaptic restriction of transsynaptic tracing from single, genetically targeted neurons. Neuron *53*, 639–647.

Zhuang, X., Masson, J., Gingrich, J.A., Rayport, S., and Hen, R. (2005). Targeted gene expression in dopamine and serotonin neurons of the mouse brain. J. Neurosci. Methods *143*, 27–32.